Journal of Scientific & Industrial Research
Vol. 70, August 2011, pp. 628-633

A greenhouse integrating desalination, water saving and rainwater harvesting for use in salt-affected inland regions

P A Davies[1]*, R K Srivastava[2], B Kaphaliya [2], A K Hossain[1], O Ngoye Igobo[1] and G Garantziotis[1]
[1] Sustainable Environment Research Group, School of Engineering and Applied Science, Aston University, Birmingham B4 7ET, UK
[2]Department of Environmental Sciences, G B Pant University of Agriculture & Technology (GBPUAT), Pantnagar, India

Received 04 May 2011; revised 03 June 2011; accepted 07 June 2011

This study proposes a new type of greenhouse for water re-use and energy saving for agriculture in arid and semi-arid inland regions affected by groundwater salinity. It combines desalination using reverse osmosis (RO), re-use of saline concentrate rejected by RO for cooling, and rainwater harvesting. Experimental work was carried at GBPUAT, Pantnagar, India. Saline concentrate was fed to evaporative cooling pads of greenhouse and found to evaporate at similar rates as conventional freshwater. Two enhancements to the system are described: i) A jet pump, designed and tested to use pressurized reject stream to re-circulate cooling water and thus maintain uniform wetness in cooling pads, was found capable of multiplying flow of cooling water by a factor of 2.5 to 4 while lifting water to a head of 1.55 m; and ii) Use of solar power to drive ventilation fans of greenhouse, for which an electronic circuit has been produced that uses maximum power-point tracking to maximize energy efficiency. Re-use of RO rejected concentrate for cooling saves water (6 l d^{-1} m^{-2}) of greenhouse floor area and the improved fan could reduce electricity consumption by a factor 8.

Keywords: Desalination, Greenhouse cultivation, Photovoltaic, Reverse osmosis (RO), Salinity

Introduction

In India (from arid and semi-arid zones of western states of Rajasthan, Haryana, Punjab and Gujarat), 25% of groundwater is affected by salt, often rendering it unfit for human consumption and marginally fit for agriculture[1,2]. In such locations, options for managing soil and groundwater salinity include: R&D efforts to select and develop salt tolerant crops, soil amendment and planting of guard crops to reduce saline water logging. Desalination of groundwater using reverse osmosis (RO) membranes is another option, but expensive, requiring specialized membranes and electricity, which may be scarcely available in agricultural areas. In future, wider uptake of RO combined with photovoltaic (PV) panels is expected due to improved availability, performance and the ever growing need for desalination. A drawback with the RO desalination process is that it rejects a stream of concentrated saline water, disposal of which is problematic in inland situations. However, this waste stream can be usefully employed for cooling as reported[3] that a cooled greenhouse (GH) provides water saving environment for plants, and PV generators power optimally designed pumps and fans to move fluid and air through the system. The concept was later partially demonstrated through laboratory studies of its components, though no GH was constructed in such studies[4].

This paper reports the first field experiment to test the idea of cooling using RO concentrate in a GH. It also describes: i) a jet pump that harnesses energy from concentrate stream and uses it to improve the performance of GH cooling systems; and ii) an improved control circuit for PV-powered ventilation fan to boost air flow and save electricity.

Experimental Section

Experimental Greenhouse (GH) at G B Pant University

A prototype pad-and-fan GH with RO system was installed at GBPUAT, Pantnagar, India. Though soil in this area is not salt affected, it provided a suitably controlled location for testing of integrated GH concept using synthetic groundwater to demonstrate feasibility of the concept of using saline water for cooling in GH, to

*Author for correspondence
E-mail: p.a.davies@aston.ac.uk

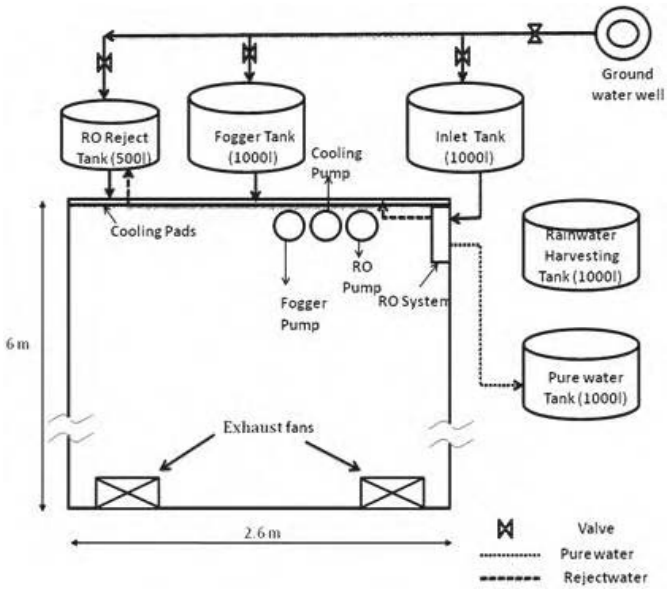

Fig. 1—Schematic of prototype greenhouse at G B Pant University, Pantnagar

study optimization of water use in cooling process and to compare the consumption between pure and saline water.

Materials and Methods

A GH (6.1 m x 3.15 m x 3 m), with a plan area (19.2 m^2), was constructed (Fig. 1) having walls and roof clad with 6 mm thick polycarbonate sheet. Evaporating cooling system consisted of pads (3.15 m x 1.2 m x 0.1 m) of plasticized cellulose paper. A digital controller was set to activate evaporative cooling when internal temperature exceeded 25°C. An automatic fogger system giving a discharge of 14 l/min was set to switch on when internal relative humidity (RH) fell below 50%. RO system had an output capacity of 50 l/h. There were 2 exhaust fans (diam, 45.7 cm each) with a 1 HP motor. There were a total of 5 water tanks outside the GH for inlet water, RO rejected concentrate, RO pure water output, water for foggers and rainwater harvested from GH roof. To determine any loss of performance to GH cooling system as a result of salinity, pure water and synthetic saline water (5000 ppm NaCl) was used as inlet water alternately (1st 4 days saline water, then 1 week pure water, then 1 week saline water, finally 1 week pure water) and water consumption was measured in each case. This experiment was carried out during October 2010 (sunshine hours, 8-10.4 h; ambient temp., 32-33°C; RH, 80-86%). Daily fluctuations of temperature and RH were measured (Fig. 2). Data of ambient temperature and RH were collected from local weather station. Water consumption for maintaining temperature and RH for proper growth of plants grown inside GH was studied.

Table 1—Optimization of consumption of water in greenhouse

Time	Volume of water in inlet tank T_1	Volume of water inRO reject water tank T_3	Volume of water in pure water tank T_2
h	l	l	l
0	1000	0	0
24	464	484	52
39	127	788	85
63	127	666	85

Results and Discussion

Inside the GH, temperature varied from 24 to 20°C and RH from 70 to 86% (Fig. 2). Initially, 1000 l water (salinity, 5000 ppm) was supplied to T_1 tank (Table 1). In the first experiment, conducted to find out the amount of pure and reject water generated per day, the cooling system was switched off and the RO system was switched on. After 24 h, volumes of water in tanks were: T_1, 464; T_2, 52; and T_3, 484 l. Minimum volume of water required in T_1 tank to run RO system is 127 l. So, water available for the RO system is only 337 l (464-127 =337 l), which is sufficient just for next 15 h. Out of 337 l, pure and reject water generated was 33 l and 304 l respectively. For the next experiment, to find out evaporation loss/ day, water available in tank T_2 and T_3 was measured as 85 l and 788 l respectively. For this experiment, the RO system was switched off, the cooling system was switched on, water remained constant in T_1 (127 l) and T_2 (85 l) tanks andonly the water available in T_3 tank (788 l) was used. It was found that on second day of this experiment (after 63 h), water level decreased from 788 l to 666 l in T_3, which shows that reduction in water level is 122 l in 24 h. So, evaporation loss in GH is 122 l/d. Similar results of water consumption in GH were obtained using pure water instead of saline water for cooling.

Jet Pump to Boost Cooling Water Flow for Evaporative Pads

Performance of evaporative pads (ht, 1.2 m) can be enhanced by use of a recirculation flow, which leads to better moistening of pads than a single pass arrangement[5]. Residual energy associated with the pressure of concentrate outlet stream of RO system can be used to induce recirculation flow. This stream can be fed to a jet pump (also called an eductor), which (Fig. 3) passes water through an orifice (diam, 1.2 mm), where it acquires high velocity and therefore low pressure, in accordance with Bernouilli's principle. High pressure water is passed into a mixing chamber, wherein a second

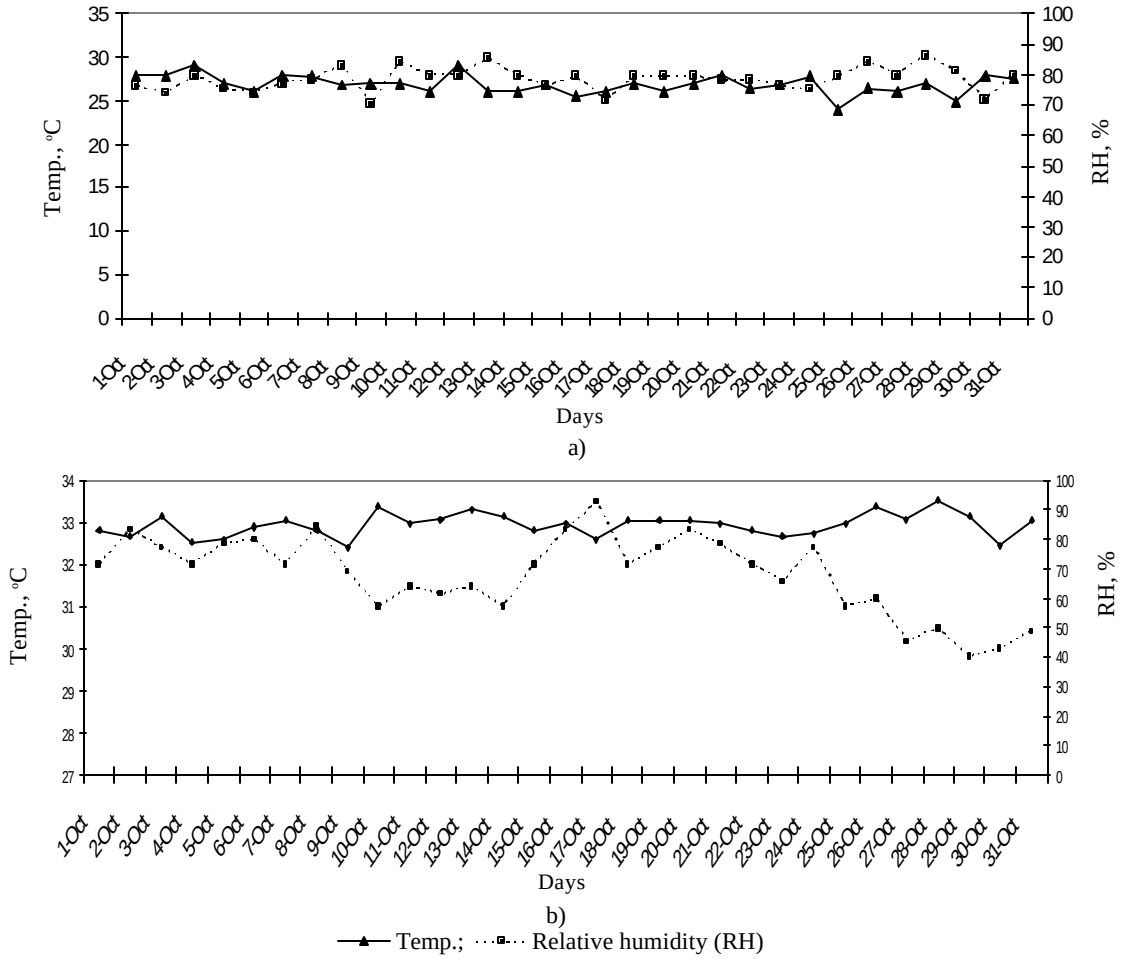

Fig. 2—Temperature and relative humidity (daily maxima) for October 2010: a) ambient; and b) inside greenhouse

stream of water is drawn by suction, before combined flow passes into a diffuser section where higher pressure is restored[6]. To demonstrate operation of jet pump at the concentrate outlet of an RO system, a pump was machined from brass stock. The diffuser section had an entrance (diam, 7.2 mm) diverging to a diameter of 22 mm with an included angle of 10 degrees. As jet pump poses a resistance to the flow of liquid, it replaces throttle valve as typically used in a RO system. Jet pump was connected to the concentrate output of a RO rig incorporating a helical rotor pump; this rig installed at Aston University (UK)[4]. Jet pump was used to raise water from a tank to an outlet at a height of 1.55 m. This will be sufficient in practice to irrigate evaporation pads. To simulate variation in power input over a typical day in April in Northern India, power into helical rotor pump was varied (80-247 W), generating a pressure (7.25-14 bar) at inlet to jet pump. At each setting, flows were measured using rotameters and by weighing of total output of jet pump over a period of 1 min. Three flows were thus recorded: (i) freshwater output of RO system; (ii) concentrate output of RO system; and (iii) augmented flow (sum of concentrate flow and additional water re-circulated by jet pump) at the outlet of the jet pump. Thus the jet pump augmented the flow (Fig. 4) by a factor of 2.5-4.0, as compared with no jet pump. Thus the jet pump enables the flow to the evaporative cooling pad to be greater by the same factor.

Improved PV Fan Controller

The GH was operated using sustainable energy obtained from a PV generator. Feasibility of running an efficient solar-powered fan using a brushless DC motor connected to PV has been demonstrated[4]. In this study, the system was improved by incorporating a maximum power point tracker (MPPT) to extract maximum available power from PV generator. Solar PV is a non-linear power generator whose output varies with solar irradiance; it has a unique point called maximum power point (MPP) on its voltage-current or voltage-power

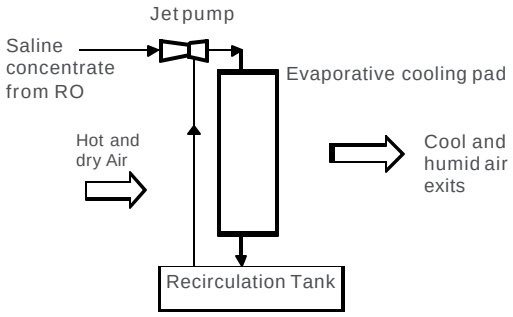

Fig. 3—Jet pump used to re-circulate saline cooling water through an evaporative cooling pad

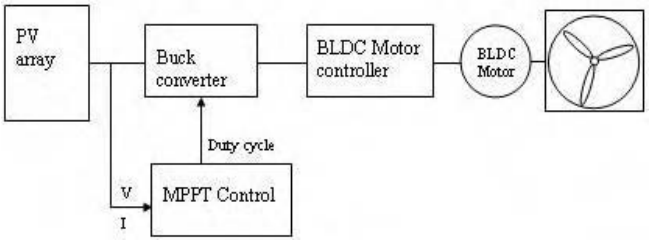

Fig. 5—Block diagram of maximum power point tracker

curve, at which system operates with maximum efficiency and produces its maximum output power. MPPT electronically tracks and varies electrical operating point of PV array, so that PV array delivers maximum available power to the load. It matches the load to PV output in spite of varying sunlight.

Theory and Design of MPPT

In PV-fan system (Fig. 5), a DC-DC buck converter (BC) interfaces PV array to load (motor), enabling electrical operating point of PV to match with that of the load under all conditions. At any given solar irradiance, power delivered to load is proporl:tional to the duty cycle of converter's PWM. At low irradiance, low duty cycle is required and *vice versa*. Thus control circuit of MPPT works by measuring PV's power and searching for optimal power point by adjusting duty cycle. BC (Fig. 6) is mainly composed of switching power MOSFET Q, flywheel diode D, inductor L and filter capacitor C. On operation, BC converts excess voltage into current, as per governing ideal equation given as $D = V_{out}/V_{mpp}$ & $I_{out} = I_{mpp} / D$, where D is duty cycle, and Vmpp and Impp are respectively input voltage and current at MPP at any given level of insolation. To provide a good compromise between noise, output switching efficiency, and permissible ripple, a switching frequency (12 KHz) is chosen. A higher frequency would allow lower inductor and capacitor values, but increase switching losses in

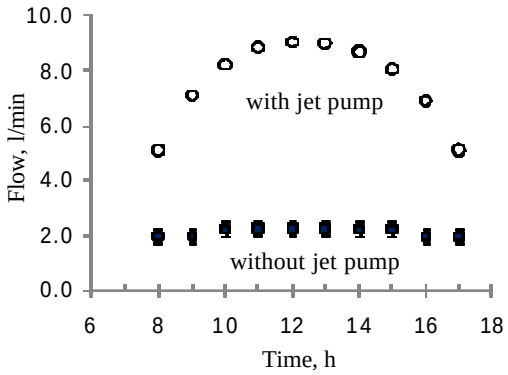

Fig. 4—Flows available for evaporative cooling system with and without assistance of jet pump added to concentrate output of RO system

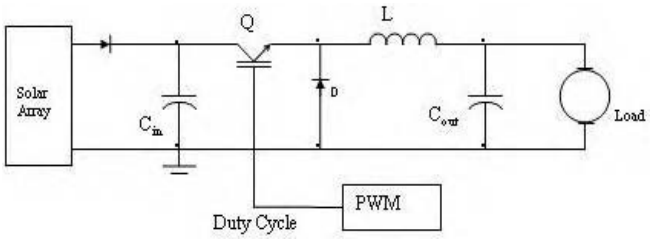

Fig, 6—Schematic of buck converter

power MOSFET and reduce tracking ability[6]. Inductor selection is based on minimum duty cycle, corresponding to the minimum solar irradiance at which the system can be operated, and is given as

$$L = \frac{V_g (V_{mpp} - V_g)}{r\, I_o\, F\, V_{mpp}} \qquad \ldots(1)$$

where, F, switching frequency; r, ripple current ratio (10-30%); and V_{mpp}, MPP voltage at minimum sun level. Also, output current, $Io = \sqrt{(V_{mpp} \times I_{mpp} \times \eta / R)}$ and voltage, $V_o = I_o R$, where, R is equivalent load resistance and η is estimated efficiency of BC [70-98% for duty cycle (0.2-1.0)].

Maximum current through inductor is equal to the sum of maximum load current plus half the ripple current, thus peak inductor current is given as $I_L = I_o + ½\ r\ I_o$. Input capacitor of a BC sees maximum ripple current (Irms_in) when duty cycle is 50% (or closest point within range to this). Output current corresponding to this is estimated as $Io = D\ V_{mpp} / R$. While input ripple current can be estimated as $I_{rms\_in} = I_o \sqrt{D\ (1 - D)}$.

The control circuit of MPPT (Fig. 7) works by measuring PV's power and searching for optimal power point by adjusting the duty cycle; this is achieved by correlating the derivative of array power with voltage

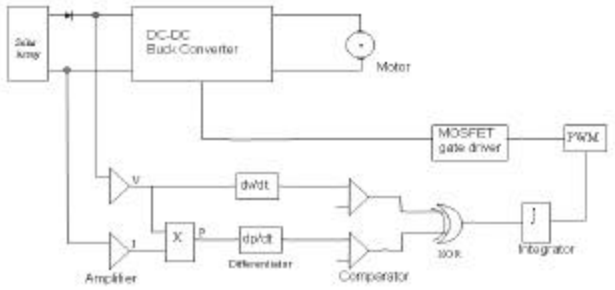

Fig. 7—Schematic of MPPT controller

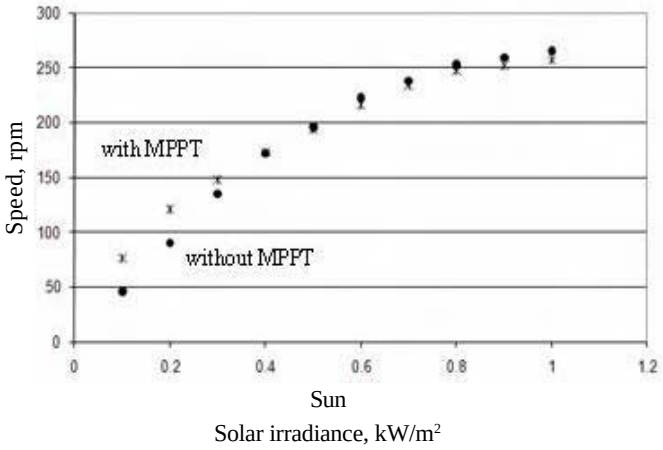

Fig. 9— Current voltage curves for PV generator at different levels of sunlight, showing direct loading and MPPT loading on various sun levels

ripple. This control algorithm is an adaptation of 'ripple correlation' techniques[7,8]. PV voltage (V) and current (I) signals are fed via amplifiers into analogue multiplier, which multiplies signals to get power (P). Differentiators are employed to obtain time derivatives (dV/dt and dP/dt) to determine the time when power and voltage is increasing or decreasing. In the next stage, comparators give output logic levels of high *(H)* or low *(L)* depending if the voltage/power is decreasing or increasing. An exclusive or-gate (X-OR) gate samples logic levels from the comparator. Integrator integrates logic level signals from X-OR gate and gives a voltage, which is incremented or decremented proportionally over time. Output of integrator is employed as the regulation signal proportional to the duty cycle of PWM, which finally controls switching duty cycle of BC.

Control logic is required to increase power to its maximum limit (Fig. 8). At the start of operation, when system/BC is switched on (point 1), the panel voltage will decrease from V_{oc}, while power will increase from zero, thus yielding dV/dt < 0 and dP/dt > 0; X-OR gate via integrator then increases duty cycle, which

dp/dt	dv/dt	Duty cycle
>0	<0	Increases
<0	<0	Decreases
>0	>0	Increases
<0	>0	Decreases

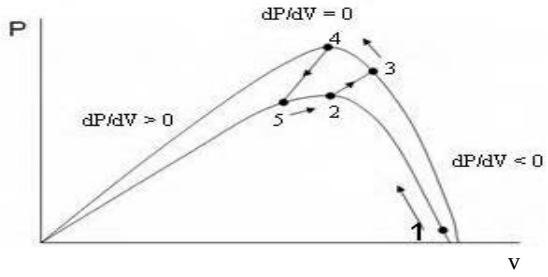

Fig. 8—Sequence of operation of MPPT on power-voltage curve of photovoltaic generator

consequently increases the power until the operating point gets to MPP (point 2). Initially at MPP point 2, an increase in sun level will shift operating point from MPP (point 2) to point 3, again yielding dP/dt > 0 and dV/dt < 0, resulting in an increase in duty cycle and subsequently increase in power until operating point gets to new MPP (point 4). Conversely, a decrease in sun level will move operating point from MPP (point 4) to point 5, where dP/dt < 0 and dV/dt < 0; X-OR gate via integrator then decreases duty cycle and consequently increases power until the new MPP is attained.

Case Study: Use of Improved PV Fan Controller at Aston University, UK

PV-fan system was set up at Aston University, UK, with a 175W BP solar panel, Vostermans Multifan 130, 3-bladed ventilation fan (diam, 1.27 m), and a 36V brushless DC motor (Delta Precision Motors 57BL116). Motor load was pre-matched to PV by coupling motor to fan via a 15:1 pulley gearing ratio, resulting in a 4 A maximum motor current at full sun. For measurement purposes, since the sun cannot be controlled, an Agilent E4306A solar array simulator was used to simulate performance of the PV array, by inputting PV parameters for 0.2 to 1 kW/m^2 solar irradiance into the simulator. Fan speed and PV output power were measured for various sun levels for: i) direct loading without MPPT; and ii) loading with MPPT. Then motor was loaded via MPPT circuit, and duty cycle was manually adjusted to ascertain tracking effectiveness.

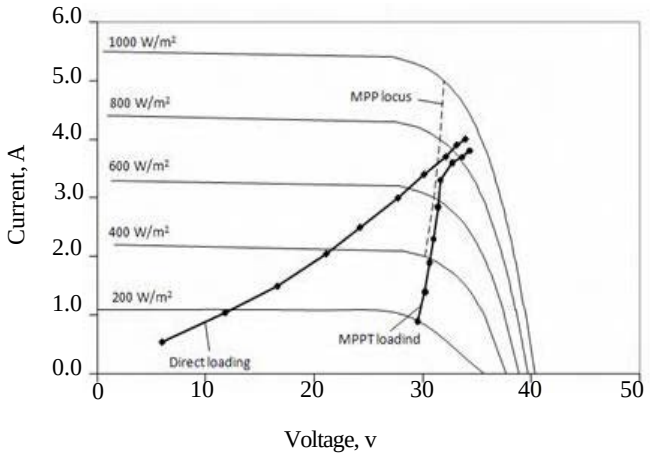

Fig. 10— Fan speed at different levels of sunlight with and without MPPT showing increased speed at low light levels

With direct loading without MPPT, power delivered to motor is along the load curve (Fig. 9), and is largely on left hand side of MPP at low sun conditions. This means that PV's optimum power is not delivered to the motor. On the other hand, when motor is connected via MPPT, power delivered to motor lies closely along MPPs locus (tracking effectiveness, 0.94-1.00) for various sun levels until the motor is saturated; then the power curve deviates along the direct loading curve. On the other hand, loading with MPPT (Fig. 10), there was a significant gain (increase in power delivered to motor) especially under low sunlight (< 0.4 kW/m^2). Highest gain (> 140%) delivered to the motor was observed at 0.1 kW/m^2 solar irradiance. Since PV-fan system's power-load was already matched for high irradiance, beyond 0.6 kW/m^2 slight losses were observed, with a maximum loss in power (3%) at 1 kW/m^2, due to losses across BC and parasitic power consumption of MPPT circuit. Manufacturers' data show that fan airflow at 260 rpm (corresponding to maximum sunlight) was 6 m^3/s.

Conclusions

Experiments with pad-and-fan GH at GB Pant University support feasibility of re-using saline water rejected from RO system for evaporative cooling. Based on rates of water consumption, no difference was noted in system behaviour when using saline water, compared to when operating with pure water. The Amount of water saved through re-use was 122 l d^{-1} in October, corresponding to the amount of water consumed in evaporative cooling pads, which conventionally require a freshwater source. This saving is equivalent to 6 l d^{-1} m^{-2} of GH floor area and can be expected to be greater in hotter, drier months. As well as conserving groundwater and making more water available for other purpose in arid areas, such re-use can contribute to management of waste concentrate rejected by RO, since evaporative cooling process reduces volume of this concentrate. Under full sunlight, PV-fan consumed 175 W, compared to 1500 W (2 HP) for the pair of mains powered fans, thus achieving an 8-fold energy saving. Another improvement comes from the application of jet pump to enable larger evaporative pads and GH areas to be cooled by the same amount of RO reject water; jet pump boosted the flow of cooling water by a factor of 2.5 to 4. Jet pump is an alternative means of recovering energy from reject stream compared to standard devices such as turbines normally used on larger RO systems. These energy efficiency measures favour the use of PV, which can provide secure power and thus facilitate cultivation of high-value crops in cooled GH environment without risk of mortality from power outages that are likely to occur with mains operation.

Acknowledgements

Authors thank Prof P K Sen and Prof P Vasudevan of IIT Delhi for facilitating this project. Funding is acknowledged from EPSRC, UK (grant reference EP/E044360/1).

References

1 Singh G, Salinity-related desertificatioin and management strategies: Indian experience, *Land Degrad & Develop*, **20** (2009) 367-385.

2 Rhoades J, Kandiah A & Mashali A, *Use of Saline Waters for Crop Production* (Scientific Publishers, Jodhpur) 1992.

3 Davies P A, Hossain A K & Vasudevan P, Stand-alone groundwater desalination system using reverse osmosis combined with a cooled greenhouse for use in arid and semi-arid zones of India, *Desalination & Water Treatment*, **5** (2009) 223-234.

4 Davies P A & Hossain A K, Development of an integrated RO-greenhouse system driven by solar photovoltaic generators, *Desalination & Water Treatment*, **22** (2010)161-173.

5 Hossain A K & Davies P A, Small-scale reverse osmosis brackish water desalting system combined with greenhouse application for use in remote arid communities, *Desalination & Water Treatment*, **3** (2009) 229-235.

6 Cunningham R, *Jet Pump Theory*, in *Pump Handbook*, edited by I Karassik, *et al* (McGraw Hill, New York) 2008.

7 Lim Y & Hamill D, Simple maximum power point trackers for photovoltaic array, *IEEE Electron Lett*, **39** (2000) 997-999.

8 Midya P *et al*, Dynamic maximum power point tracker for photovoltaic applications, in *27th IEEE Power Electronics Specialists Conf (Bavena, Italy)*, **vol 2** (1996) 1710-1716.